



## Cavitating flow around a scaled-down model of guide vanes of a high-pressure turbine



Mikhail V. Timoshevskiy<sup>a,b</sup>, Sergey A. Churkin<sup>a,b</sup>, Aleksandra Yu. Kravtsova<sup>a,b</sup>,  
Konstantin S. Pervunin<sup>a,b,\*</sup>, Dmitriy M. Markovich<sup>a,b,c</sup>, Kemal Hanjalić<sup>a,d</sup>

<sup>a</sup> Department of Scientific Research, Novosibirsk State University, 2, Pirogov Str., Novosibirsk 630090, Russia

<sup>b</sup> Kutateladze Institute of Thermophysics, Siberian Branch of the Russian Academy of Sciences, 1, Lavrentyev Ave., Novosibirsk 630090, Russia

<sup>c</sup> Institute of Power Engineering, Tomsk Polytechnic University, 30, Lenin Ave., Tomsk 634050, Russia

<sup>d</sup> Department of Chemical Engineering, Delft University of Technology, 136, Julianalaan, Delft 2628 BL, The Netherlands

### ARTICLE INFO

#### Article history:

Received 10 March 2015

Revised 21 July 2015

Accepted 19 September 2015

Available online 13 October 2015

#### Keywords:

Cavitation

Attached/cloud cavities

System/intrinsic instabilities

Asymmetric cavity length oscillations

Cross instability

Guide vane

NACA0015

High-speed visualization

PIV

### ABSTRACT

We studied cavitating flow over the suction side of two symmetric 2D foils – a NACA0015 hydrofoil and a scaled-down model of high-pressure hydroturbine guide vanes (GV) – in different cavitation regimes at several attack angles. High-speed imaging was used to analyze spatial patterns and time dynamics of the gas-vapor cavities, as well as for evaluating the characteristic integral parameters. A PIV technique was applied to measure the velocity fields and its fluctuations, which were compared for both foils and with the data measured in the non-cavitating flows at the same flow conditions. We compare the dynamics of growth and convection of traveling bubbles at a smaller attack angle and the transition of a sheet cavity pattern to a streaky one at the higher incidence on both foils. For the GV, asymmetric spanwise variations of the sheet cavity length were for the first time visualized for an unsteady regime that is characterized by alternating periodic detachments of clouds between the sidewalls of the test channel and Strouhal number of 0.27. According to numerical calculations by Decaix and Goncalvès (2013), this asymmetric behavior is very likely to be governed by the cross instability. Moreover, it was concluded that the existence of the cross instability is independent on the test body shape and its aspect ratio. For single-phase flow and cavitation inception conditions, the PIV measurements revealed the appearance of the second maximum in the fluctuating velocity distributions over the GV profile at the higher incidence angle due to the flow separation from its surface at roughly 71% of the chord length from the foil leading edge. This results in a more intensive turbulent wake past the GV compared to that behind the NACA foil. After the transition to unsteady regimes, both maxima of the fluctuating velocity over the GV vanish, the distributions become more flat and almost coincide for both foils. While at developed cavitation regimes the main flow features and cavitation dynamics do not differ much for the both foils, the detected second maximum of the fluctuating velocity for the GV at the higher attack angle makes this profile less suitable (from the hydrodynamics standpoint) for flow control in practical full-scale conditions, especially at subcavitating and cavitation inception regimes, than the NACA hydrofoil.

© 2015 Elsevier Ltd. All rights reserved.

### Introduction

Unsteady cavitation phenomena in hydropower systems are known to be one of the major sources of instabilities and mechanical damage. Especially prone to cavitation are the guide vanes of supply ducts, runner blades and draft tubes of hydroturbines. Apart from omnipresent erosion, cavitation is not regarded as dangerous as

long as its dynamics is stable. However, cavitation causes flow instabilities, pulsations and other forms of local and bulk unsteadiness, which disrupt the system operation and diminish the energy conversion efficiency. The flow unsteadiness inevitably leads to structural instabilities, load imbalance, noise and vibration of the equipment elements, their fatigue and eventual permanent damage. The consequences can be the machine failure or, in the worst cases, emergency situations. Preventing or at least diminishing and controlling cavitation and other causes of instabilities in full-scale hydropower systems has long been the primary concern of designers and operators.

Two main classes of partial cavity instabilities are distinguished (Callenaere et al., 2001): intrinsic and system (or transitional in classification by Watanabe et al., 2001). If instability originates in the

\* Corresponding author at: Kutateladze Institute of Thermophysics, Siberian Branch of the Russian Academy of Sciences, 1, Lavrentyev Ave., Novosibirsk 630090, Russia. Tel.: +7 383 3356684; fax: +7 383 3356684.

E-mail address: [pervunin@itp.nsc.ru](mailto:pervunin@itp.nsc.ru), [konstantin.pervunin@gmail.com](mailto:konstantin.pervunin@gmail.com) (K.S. Pervunin).

cavity itself, it is of intrinsic type. If it is caused by interaction of the cavity with other cavities or elements of the hydraulic system, especially inlet and outlet ducts, it is system dependent. For example, cloud cavitation occurs because of the development of an intrinsic instability – a re-entrant jet underneath the sheet cavity (e.g., see (Kawanami et al., 1997; Kubota et al., 1989; Pham et al., 1999)). The thickness of the re-entrant jet and its velocity are determined by an adverse pressure gradient. If the pressure gradient is strong enough to force the re-entrant jet to impinge upon the cavity detachment region (i.e., close to the cavity leading edge), the attached cavity interface breaks up over the whole foil span and a cloud cavity appears, which is then convected downstream by the primary flow. Cloud cavitation was a focus of many previous studies (see Callenaere et al., 2001; Huang et al., 2013; Kubota et al., 1989) and its dynamics along with the mechanism leading to its occurrence are widely discussed and well known.

The most general case of system instabilities is the so-called cavitation surge that prevails for relatively long and thin cavities (typically when the cavity length is about 75–100% of a foil chord) on single hydrofoils (Callenaere et al., 2001; Kawakami et al., 2008; Watanabe et al., 2001) or in more complex conditions (Duttweiler and Brennen, 2002; Iga et al., 2011). According to Callenaere et al. (2001), the mechanism of this instability is as follows. A minor pressure drop at a cavity location makes its volume increase and, as a result, hydraulic resistance grows. To counterbalance this, the flow decelerates at the inlet duct, which makes the local pressure gradually grow and the cavity volume decreases. When the cavity reaches its minimum length, local velocity on the contrary increases maximally that leads again to a local pressure drop. Afterwards, the process repeats and the system as a whole oscillates at a certain frequency. Thus, when cavitation surge conditions are fulfilled, the mechanism of the cavity length pulsations is driven by propagation of pressure waves along the test channel. It is also worth to note that both types of the cavitation instabilities are closely associated with quasi-periodic pulsations of the local pressure but they are the main source of unsteadiness in case of the cavitation surge and only a consequence of shedding process in case of cloud cavitation.

Despite the fair understanding of the basic physics and mechanisms of running processes, as well as the development of means and methods for diminishing and controlling cavitation, the availability of established recommendations and protocols for smooth operation and maintenance, a wide range of issues still remain, differing from one plant to another and depending on the type of machinery, their size, operation conditions and schedule. One of the issues that motivated the present work is the public unavailability of detailed research data for the full-scale equipment. Most accessible research data have been obtained in laboratories (or, more recently, by computer simulations) on generic shapes – foils, vanes, runners, ducts, which usually differ in one way or another from the proprietary bodies used in real systems. Thus, questions often posed are: how the cavity patterns on real-size guide vanes and runner blades match those on laboratory model bodies (e.g., NACA series hydrofoils), what kind of instabilities govern cavity behavior, what are the features of the flow structure around the vanes and blades compared to the standard-shaped foils?

It is recalled that despite a relatively large set of common attributes, cavitating flows around bodies of quite similar shapes and the same size can have different features. While the literature on cavitation on generic symmetric bodies is quite extensive (e.g., Foeth et al., 2008; Franc and Michel, 1985; Ji et al., 2015), some covering even subtle details on the spatial distributions of the mean and turbulence characteristics (e.g., Astolfi et al., 2000; Huang et al., 2013; Kubota et al., 1989), the data of comparative contents and their extent for realistic shapes of machine and equipment elements such as guide vanes and/or rotor blades, are scarce. New investigations are particularly needed in cases when the test body is a foil shaped to

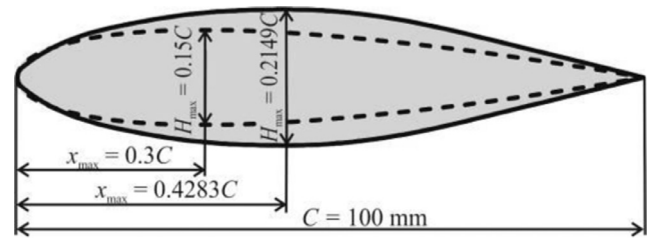


Fig. 1. Scheme of the test bodies: a NACA0015 series hydrofoil (dashed line) and scaled-down model of a guide vane (solid line). Maximum thicknesses are 15 and 21.49 mm at distances of 30 and 42.83 mm from the leading edge for the NACA foil and GV model with 100 mm chord length, respectively. The rounding radius of the leading edge is 2.48 mm for the NACA0015 foil and 1.97 mm for the guide vane model.

mimic a 2D vane or a 3D blade (even for scaled-down models) of real full-scale hydraulic machinery.

The main requirement to guide vanes in the distributors of real hydraulic units is that they must be free from flow separation and that the turbulent wake behind them must be as weak as possible at various operating conditions. In high-pressure turbines, two regular shapes of guide vanes are employed: symmetric and asymmetric. If the wrapping angle of the turbine spiral case is less than  $270^\circ$ , the simplest vanes with a symmetric hydrofoil shape are better to use. Guide vanes with an asymmetric profile are mounted in turbines for which the wrapping angle of spiral case is about  $360^\circ$ .

In this paper, a scaled-down model of guide vanes with a symmetric cross-section used in high-pressure hydroturbines is considered. We report here on a visual analysis of high-speed imaging of spatial structure and dynamics of gas-vapor cavities and the thereof deduced integral characteristics, as well as on PIV measurements of spatial distributions of velocity and its turbulent fluctuations around the cavitating guide vane model. The results are compared with those for a well-studied NACA0015 series hydrofoil with the same chord length.

## Experimental conditions and measurement techniques

The experiments were carried out in the Cavitation tunnel in Kutateladze Institute of Thermophysics SB RAS. Its description as well as details on the experimental conditions and measurement techniques applied can be found in (Kravtsova et al., 2014). A scaled-down model of a guide vane (GV) and a NACA0015 hydrofoil, placed in the tunnel test section, were subjected to different cavitation numbers  $\sigma = (P_{in} - P_V)/(\rho U_0^2/2)$ , where  $P_{in}$  and  $P_V$  are the static pressure at the test section inlet and the water vapor pressure, respectively,  $\rho$  is water density and  $U_0$  is the mean (bulk) flow velocity. Cavitation number was controlled by varying the mean flow velocity, which was chosen to achieve a range of targeted cavitation regimes. Three attack angles have been considered for both bodies,  $\alpha = 0, 3$  and  $9^\circ$ . Both test bodies, which are two-dimensional symmetric foils (Fig. 1), were made of brass with the same surface roughness of  $1.5 \mu\text{m}$ . Their chord length  $C$  is 100 mm. The maximum width of GV is  $H_{max} = 0.2149C$  measured at the distance of  $x_{max} = 0.4283C$  from the leading edge. The GV profile was constructed as a cubic spline approximation of the points given in Table 1. Its shape practically replicates the one of the NACA 65-021. The aspect ratio (the ratio of the foil span to its chord) for both foils was  $AR = 0.8$  that is very close to the one in some practical full-scale conditions.

## Results

We present below some results of the experimental investigation of cavitating flows over the GV and NACA0015 foil for two attack angles,  $\alpha = 3^\circ$  and  $9^\circ$  at different regimes defined by the cavitation number. The presentation begins with a discussion of selected images from high-speed visualization and thereof deduced integral

Download English Version:

<https://daneshyari.com/en/article/7060309>

Download Persian Version:

<https://daneshyari.com/article/7060309>

[Daneshyari.com](https://daneshyari.com)